JOURNAL OF SOLID STATE CHEMISTRY **41**, 114–123 (1982)

The Phase Relationship among Compounds $Ba_{1+x}Fe_2S_4$

J. S. SWINNEA AND H. STEINFINK

Materials Science and Engineering Laboratories, Department of Chemical Engineering, The University of Texas at Austin, Austin, Texas 78712

Received July 20, 1981; in revised form September 21, 1981

The dependence of composition of the phases $Ba_{1+x}Fe_2S_4$ on sulfur vapor pressure and starting composition was investigated at 650, 747, and 800°C. The infinitely adaptive series $Ba_{1+x}Fe_2S_4$ spans the compositions $0.072 \leq x \leq 0.142$. The value of x decreases as the sulfur vapor pressure increases at a given temperature. Varying the ratio of Ba/Fe in the starting mixture has no effect on the $Ba_{1+x}Fe_2S_4$–sulfur fugacity relationship. The phase $BaFe_2S_4$ is not part of the infinitely adaptive series.

Introduction

The investigation of the Ba–Fe–S system has led to the discovery of a series of phases with the general formula $Ba_{1+x}Fe_2S_4$ or $Ba_p(Fe_2S_4)_q$ which fit the criteria for "infinitely adaptive series" as proposed by Anderson (*1*). Detailed analyses for several members of the $Ba_p(Fe_2S_4)_q$ series have led to postulated crystal structures for all possible values of p and q (*2, 3*). The basic structure consists of two subcells, the first being a rigid chain of edge-sharing Fe–S tetrahedra parallel to the c axis while the second is formed from a chain of Ba atoms situated in the channels formed by the S atoms. Grey's early attempts (*4*) to prepare various members of the $Ba_{1+x}Fe_2S_4$ series involved linking the composition, or value of x, with reaction temperature and excess sulfur in the reaction mixture. The barium-to-iron molar ratio in the starting mixture was kept constant at 1 : 2 while the barium-to-sulfur molar ratio was varied in the range from 1 : 4 to 1 : 6. The mixtures were heated at temperatures ranging from 540°C to 800°C for 1 to 4 days and then quenched in water. This procedure is subject to several limitations. It does not lend itself to a systematic investigation of the system variables, and reaction temperature, starting composition, and reaction time are varied simultaneously. The sulfur pressure, and thus the sulfur activity, remains uncontrolled, indeed is unknown, because the pressure in the reaction tube will depend on the free volume in the tube. Since the pressure was not controlled, quantitative information on the dependence of x on sulfur pressure could not be extracted from these results, and Grey stated that more detailed work with control of both sulfur pressure and temperature would be required to obtain a full understanding of the thermodynamic properties of this region of the Ba–Fe–S phase diagram.

We undertook a systematic study in which the sulfur vapor pressure, reaction temperature, and composition were controlled separately, and preliminary results were published recently (*5*). While this work was in progress, Nakayama *et al.* (*6*)

0022-4596/82/020114-10$02.00/0

published a study on this series of compounds which was a slightly modified repetition of Grey's work and it incorporated the same disadvantages of not individually controlling the variables, especially the sulfur pressure. In this investigation the dependence of the system on sulfur vapor pressure and starting composition at three reaction temperatures, 650, 747, and 800°C, is examined. These three isotherms were chosen because FeS_2 (pyrite) decomposes into $Fe_{1-x}S$ (pyrrhotite) and S_{liq} at 742°C. Thus, the 650°C isotherm represents a region in equilibrium with sulfur vapor, the 747°C isotherm occurs near the decomposition point, and the 800°C isotherm includes a liquid sulfur phase as well.

Experimental

BaS, Fe, and S constituted the starting materials for the preparation of $Ba_{1+x}Fe_2S_4$. Commercial, yellow BaS, containing free sulfur, was heated at 600°C for 2 days under a current of H_2 in argon to remove the free sulfur. After treatment, the X-ray powder diffraction pattern of the now white BaS showed no extraneous lines. The Fe powder (Alfa Inorganic) and the S powder (Atomergic Chemicals) were of 3N and 5N purity, respectively. The BaS and Fe powders were weighed to ±0.1 mg to give specific ratios of Ba : Fe and after mixing were contained in loosely capped graphite tubes. These tubes were placed at one end of Vycor tubes about 25 cm long and excess sulfur was placed at the other end. They were sealed under a vacuum of 10^{-3} to 10^{-4} mm Hg. The sealed tubes were placed in a horizontal furnace with the BaS and Fe mixture at a constant temperature, T_h, and the sulfur at a lower temperature, T_c, to provide a constant sulfur pressure in the tube. The two temperatures were continuously monitored by digital pyrometers which had ±2°C precision. After 2 days the samples were quenched in water.

X-Ray powder diffraction patterns of the reacted samples were obtained using a Philips diffractometer fitted with a diffracted beam graphite monochromator and Cu$K\alpha$ radiation. This instrument was frequently calibrated by observation of the (111) reflection of a silicon single crystal. Scans at $\frac{1}{4}$° 2θ/min of several peaks of the normally highly crystalline $Ba_{1+x}Fe_2S_4$ samples were taken to determine the stoichiometries of these phases. Values of x for $Ba_{1+x}Fe_2S_4$ were obtained from X-ray powder diffraction patterns by indexing the $10p$, 200, $21q$, $21p$, and 220 reflections (*4*). The precision of measurement for the diffraction lines was about ±0.02° 2θ or about 0.0007 in $\sin^2\theta$ yielding a precision in the determination of x of ±0.002.

The vapor pressure of sulfur, a complex mixture of species S_i ($i = 1, 2, \ldots, 8$) whose relative proportions vary with sulfur pressure and temperature, is fairly well known from about 100°C to its critical point. One of the more recent studies was done by Mills (*7*), who derived the following expression for the vapor pressure from 370 to 1313°K:

$$\log P(\text{atm}) = -6109.6411\, T^{-1} + 16.64157 - 0.01705358\, T + 7.9769 \times 10^{-6} T^2.$$

The equilibrium constants for the gaseous sulfur species $S_n(g) \rightleftarrows (n/2)S_2(g)$ can be obtained from the relation

$$\log K = AT^{-1} + B + C \log T \; (T = {}^\circ\text{K})$$

and we used the constants listed by Mills (*7*). The partial pressures of all species can thus be calculated at any pressure and temperature. When pressures are high, partial pressures must be modified with fugacity coefficients to calculate sulfur fugacities which are directly related to sulfur activities. The theory of corresponding states applies well to sulfur even though it is a complicated mixture of different molecules, because the value of the critical compression factor Z_c is quite normal; it is known that mixtures of chemically similar molecules behave very much like ideal mixtures and the nonexistence of specific interactions between different but similar sulfur species is probably a good assumption (*8*) and permits the use of

$$\phi(S_1) = \phi(S_2) = \cdots = \phi(S_8) = \phi(P_{\text{total}}).$$

The fugacity coefficients were calculated using the generalized coefficient equation (*9*)

$$\ln \phi = \frac{P_r}{T_r}(B^0 + \omega B^1),$$

where $B^0 = 0.083 - 0.422/T_r^{1.6}$; $B^1 = 0.139 - 0.172/T_r^{4.2}$; $T_r = T/T_c$; $P_r = P/P_c$, and ω = Pitzer acentric factor, 0.070. The total pressure is given by the sum of the partial pressures of all the species, $P = \sum_{i=1}^{8} P(S_i)$. The equilibria $S_i = (i/2)S_2$ are given by the equilibrium constants

$$K_i = \frac{P(S_2)^{i/2}\phi^{i/2}}{P(S_i)\phi}$$

so that

$$P = \sum_{i=1}^{8} \frac{\phi^{(i/2-1)}P(S_2)^{i/2}}{K_i},$$

where $K_2 = 1$. A computer program was written which calculates these fugacities using a Newton–Raphson iterative procedure.

Pyrrhotite, $Fe_{1-x}S$, is one of the phases in equilibrium with $Ba_{1+x}Fe_2S_4$ and its compositional dependence on T and P has been carefully evaluated by Rau (*10*). The compositions $Fe_{1-x}S$ can be calculated as functions of T and sulfur fugacity by use of energetic parameters of the defect structure. We used Rau's equations modified for the condition that no iron exists on S sites under our experimental conditions. This yields the equations

$$r = 1/(1 - [V_{Fe}]),$$

$$a_s = [V_{Fe}] \exp\{(\mu(FeS) + g(V_{Fe}))/RT\} \times \exp\{4\,\xi(V_{Fe})[V_{Fe}](2 - [V_{Fe}])/RT\},$$

where μ(FeS) is the free energy of formation of stoichiometric FeS from the elements, $g(V_{Fe})$ is the free energy of formation of an iron vacancy by removing one atom of iron from the lattice to solid iron, $\xi(V_{Fe})$ is the free energy of interaction of these vacancies, r is the atomic ratio of sulfur/iron, $[V_{Fe}]$ is the mole fraction of the Fe vacancy, and a_s is the activity of elemental sulfur. The values we used for these parameters were calculated from

$$(\mu(FeS) + g(V_{Fe}))/RT = 10.508 - 16{,}348/T$$

$$4\,\xi(V_{Fe})/RT = 3.160 + 22{,}269/T.$$

The maximum sulfur content of pyrrhotite at any temperature can be read from the phase diagram in Rau (*10*) and can then be converted to limiting sulfur fugacities using the equations just presented. For the 650°C isotherm a maximum sulfur content of 54.3 atom% is found. This corresponds to a sulfur-to-iron ratio of 1.188 or the phase $Fe_{0.842}S$, and the limiting sulfur fugacity is 0.11 atm. Above this fugacity $Fe_{0.842}S$ is in equilibrium with FeS_2 (pyrite). At 747°C the maximum sulfur content is 54.8 atom% which corresponds to $r = 1.214$ or $Fe_{0.824}S$. The limiting sulfur fugacity is 5.76 atm, and above this fugacity $Fe_{0.824}S$ is in equilibrium with liquid sulfur. Finally, at 800°C the maximum sulfur content is 54.8 atom% or $r = 1.213$. Thus, above the calculated limiting sulfur fugacity of 10.71 atm, $Fe_{0.825}S$ is in equilibrium with liquid sulfur. It is assumed in these calculations that the presence of a second solid phase will not influence the $Fe_{1-x}S$-$f(S_2)$ equilibria as determined by Rau.

Results

A summary of the results is presented in Tables I and II, which list reaction conditions and products which were identified

TABLE I

Reaction Conditions and Products for $Ba_{1+x}Fe_2S_4$ Preparations at 650, 747, and 800°C and Constant Ba–Fe Ratios

T_c (°C)	$f(S_2)$ (atm × 10^2)	$f(S)_{total}$ (atm × 10^2)	Products x	 Fe/S	 Others
T_H = 650°C Ba/Fe = 1.000/2.000					
588	192	578	0.0000		$FeS_2 + BaS_3$
581	187	536	0.0000		$FeS_2 + BaS_3$
371	26.7	30.3	0.0750	0.842	FeS_2
368	25.1	28.4	0.0757	0.842	FeS_2
361	22.5	25.1	0.0761	0.842	FeS_2
336	14.1	15.3	0.0909	0.842	FeS_2
325	11.2	12.0	0.0814	0.8418	
312	3.4	9.0	0.0885	0.8445	
267	2.70	2.80	0.1031	0.8552	
263	2.41	2.49	0.0938	0.8563	
254	1.82	1.87	0.1034	0.8589	
252	1.74	1.76	0.0977	0.8593	
240	1.19	1.22	0.0925	0.8628	
233	0.94	0.96	0.0945	0.8650	
195	0.22	0.22	0.1116	0.8781	
169	0.069	0.070	0.1239	0.8883	
134	0.010	0.010			$BaFe_2S_3$
T_H = 747°C Ba/Fe = 1.000/2.000					
610	481	742	0.0000	0.8236	
499	175	206	0.0771 + 0.00	0.8343	
458	107	120	0.0712 + 0.00	0.8395	
438	81.9	90.2	0.0722 + 0.00	0.8422	
421	64.3	69.9	0.0946	0.8447	
381	34.1	36.2	0.0990	0.8512	
337	15.0	15.6	0.1012	0.8595	
293	5.52	5.65	0.1066	0.8693	
254	1.87	1.90	0.1143	0.8798	
210	0.41	0.42	0.1255	0.8940	
174	0.088	0.089	0.1341	0.9080	
141	0.016	0.016	0.1440	0.9230	
T_H = 800°C Ba/Fe = 1.000/2.000					
636	726	988	0.0700 + 0.00	0.8289	
621	639	840	0.0700 + 0.00	0.8303	
598	520	654	0.0803 + 0.00	0.8326	
527	254	291	0.0720 + 0.00	0.8403	
507	203	228	0.0655 + 0.00	0.8428	
469	128	139	0.0782	0.8477	
435	80.6	86.4	0.0860	0.8525	
359	23.3	24.2	0.0914	0.8654	
298	6.28	6.40	0.1081	0.8787	
245	1.42	1.43	0.1368	0.8932	$BaFe_2S_3$
243	1.3	1.30	0.1349	0.8938	$BaFe_2S_3$
200	0.28	0.28	0.1400	0.9085	$BaFe_2S_3$
155	0.034	0.034	0.1401	0.9272	$BaFe_2S_3$
154	0.032	0.032	0.1401	0.9277	$BaFe_2S_3$

TABLE II

Reaction Conditions and Products for $Ba_{1+x}Fe_2S_4$ Preparations at 800°C with Variable Ba–Fe Ratios

T_c (°C)	$f(S_2)$ (atm × 10^2)	$f(S)_{total}$ (atm × 10^2)	Products		
			x	Fe/S	Others
Ba/Fe = 1.100/2.000					
614	601	779	0.072 + 0.000		
558	353	418	0.0700 + 0.000		
474	136	149	0.0864		
451	101	109	0.0813		
426	70.7	75.5	0.0857		
416	60.9	64.7	0.0809		
413	58.2	61.8	0.0829		
401	48.3	50.9	0.0917		
391	41.0	43.1	0.0887		
236	1.06	1.06	0.1390	0.8960	$BaFe_2S_3$
140	0.015	0.015			$BaFe_2S_3$
Ba/Fe = 1.135/2.000					
246	1.46	1.48	0.1061		
245	1.42	1.43	0.1120		
245	1.42	1.43	0.0958		
230	0.86	0.87	0.1273		$BaFe_2S_3$
226	0.75	0.75	0.1322		
225	0.72	0.73	0.1114		
221	0.62	0.63	0.1367	0.9010	
Ba/Fe = 0.500/2.000					
366	26.5	27.6	0.0966	0.8641	
Ba/Fe = 0.250/2.000					
399	46.7	49.3	0.0954	0.8582	
Ba/Fe = 1.250/2.000					
457	109	118	0.0720 + 0.000	0.8494	

for each reaction. Values of x listed for products refer to x in $Ba_{1+x}Fe_2S_4$ and Fe/S refers to the Fe/S ratio in any $Fe_{1-x}S$ (pyrrhotite) phase found to be in equilibrium with $Ba_{1+x}Fe_2S_4$.

At 650°C the equilibrium properties of $Ba_{1+x}Fe_2S_4$ show three distinct regions (Fig. 1). The starting composition of Ba/Fe = 1 : 2 is indicated by the dashed line. Below an S_2 fugacity of about 1×10^{-1} atm a definite value of x for each fugacity is in equilibrium with small quantities of pyrrhotite which vary in composition between $Fe_{0.842}S$ and $Fe_{0.888}S$. The $Ba_{1+x}Fe_2S_4$ phases in this region range from $x = 0.075$ to $x = 0.124$ with x decreasing with increasing sulfur fugacity. When the fugacity falls to about 1×10^{-4} atm $f(S_2)$ only $BaFe_2S_3$ appears in the reacted mixture. From about 1×10^{-1} atm $f(S_2)$ to about 1.0 atm $f(S_2)$ the reaction products include $Ba_{1.075}Fe_2S_4$, $Fe_{0.842}S$, and FeS_2(pyrite). Finally, above an S_2 fugacity of about 1.0 atm, $Fe_{0.842}S$ disappears, and FeS_2, stoichiometric $BaFe_2S_4$ and BaS_3 are in equilibrium.

The 747°C isotherm (Fig. 2) was investigated from a minimum S_2 fugacity of 1.6×10^{-4} atm to an upper S_2 fugacity of approximately 5 atm at a starting composition of Ba/Fe = 1 : 2 shown by the dashed line.

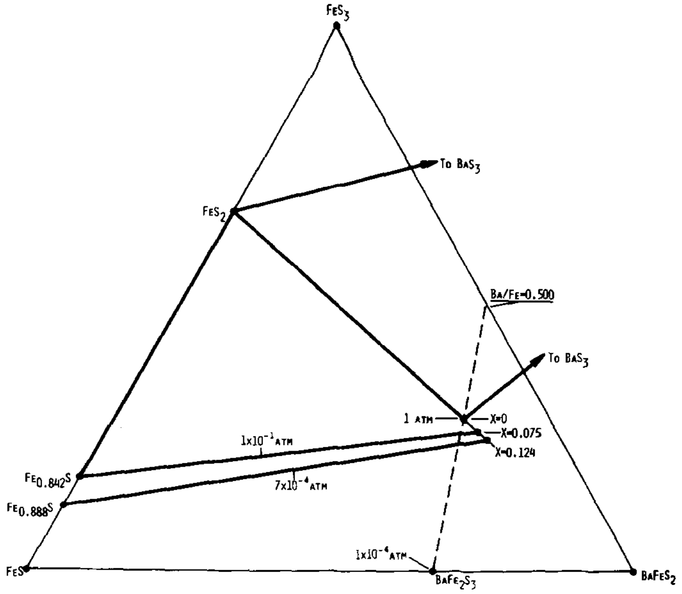

FIG. 1. Phase diagram for $Ba_{1+x}Fe_2S_4$ at 650°C. Starting composition for Ba/Fe is shown by dashed line.

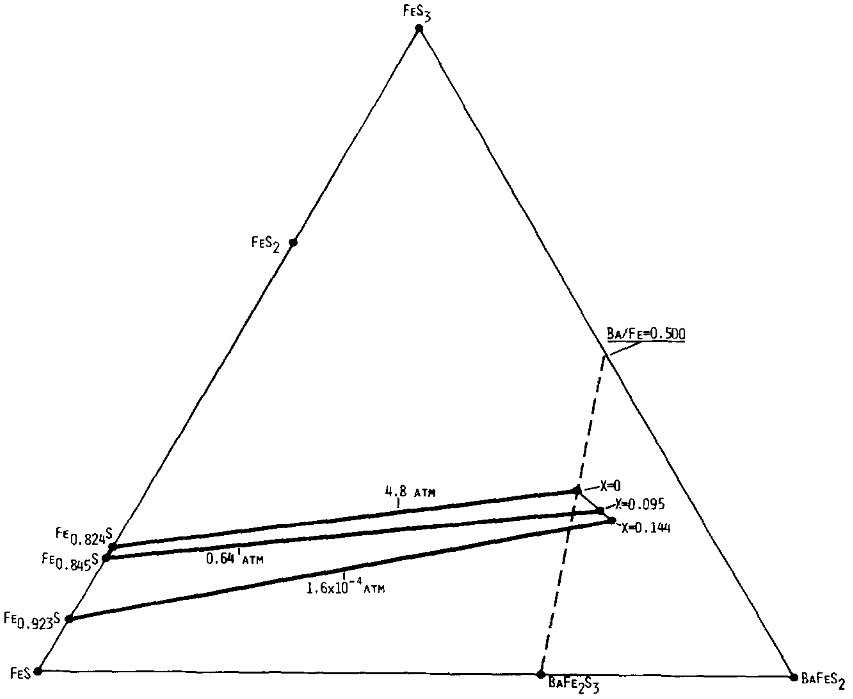

FIG. 2. Phase diagram for $Ba_{1+x}Fe_2S_4$ at 747°C. Starting composition is shown by the dashed line.

From 1.6 × 10^{-4} atm $f(S_2)$ to just about 0.64 atm $f(S_2)$ a definite value of x at each fugacity is in equilibrium with small amounts of pyrrhotite which vary in composition between $Fe_{0.923}S$ and $Fe_{0.839}S$. The $Ba_{1+x}Fe_2S_4$ phases in this region range from $x = 0.095$ to $x = 0.144$ with x decreasing with increasing sulfur fugacity. In Table I are shown the results of three experiments at S fugacities of 0.82, 1.07, and 1.75 atm. At these pressures $Ba_{1.072}Fe_2S_4$, $BaFe_2S_4$, and $Fe_{1-x}S$, x varying between 0.842 and 0.834, were the observed phases. Thus, between 0.64 and 0.82 atm a tie line between $Ba_{1.072}Fe_2S_4$ and the corresponding $Fe_{1-x}S$ phase, $0.842 \leq x \leq 0.845$, exists. At about 4.8 atm $f(S_2)$ on the Fe–S diagram a maximum in the sulfur content of pyrrhotite is reached at $Fe_{0.824}S$. At higher fugacities this pyrrhotite phase is accompanied by a liquid sulfur phase. At 4.8 atm only single phase, stoichiometric $BaFe_2S_4$ is observed in the reaction product.

At 800°C the behavior is very similar to that at 747°C. In Fig. 3 the starting composition Ba/Fe = 1:2 is represented by a dashed line. At an S_2 fugacity of approximately 1.5 × 10^{-4} atm only single-phase $BaFe_2S_3$ is observed. From 1.5 × 10^{-4} atm $f(S_2)$ to 0.014 atm $f(S_2)$, $Ba_{1+x}Fe_2S_4$, x about 0.14, exists in equilibrium with $BaFe_2S_3$ and small amounts of pyrrhotite which vary in composition from $Fe_{0.934}S$ to $Fe_{0.894}S$. A definite value of x at each fugacity and small amounts of pyrrhotite with no $BaFe_2S_3$ are in equilibrium from 0.014 atm $f(S_2)$ to 1.3 atm $f(S_2)$. In this region x varies from 0.078 to 0.14 and the composition of the pyrrhotite phases varies from $Fe_{0.894}S$ to $Fe_{0.848}S$. Finally, from an S_2 fugacity of about 1.3 atm to the maximum S_2 fugacity studied, 6.3 atm, $BaFe_2S_4$ is in equilibrium with $Ba_{1.078}Fe_2S_4$ and a small amount of pyrrhotite varying from $Fe_{0.848}S$ to $Fe_{0.830}S$. One can expect to make only single-phase $BeFe_2S_4$ at the point in the Fe–S diagram

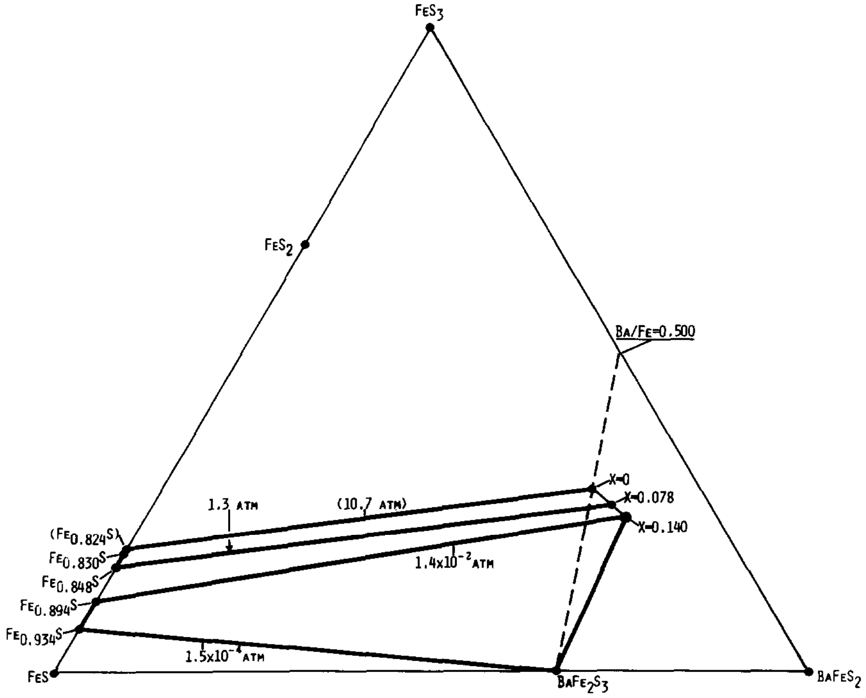

FIG. 3. Phase diagram for $Ba_{1+x}Fe_2S_4$ at 800°C. Starting composition is indicated by dashed line.

at which the pyrrhotite sulfur content reaches a maximum, as was observed at 747°C. At 800°C this maximum occurs at 54.81 atom% S or $Fe_{0.824}S$ and requires an S_2 fugacity of approximately 10.7 atm or a total sulfur pressure of 18.7 atm! This pressure was not experimentally obtainable using sealed Vycor tubes, which can be used only to pressures of about 10 atm, but it is indicated in parentheses as the speculative limit on the phase diagram.

All of the above isotherms used a starting composition with a Ba : Fe ratio of 1.000 : 2.000, and so most of the reaction products were multiphase, containing pyrrhotite with the $Ba_{1+x}Fe_2S_4$ phases. In order to prepare single-phase $Ba_{1+x}Fe_2S_4$ for use in physical property measurements and to investigate the $Ba_{1+x}Fe_2S_4$ series at another starting composition, a complete isotherm with a starting composition of Ba/Fe = 1.100/2.000 was explored for 800°C. The results for this starting composition exhibit the same fugacity-equilibrium phase regions as those previously described. Although the $Ba_{1+x}Fe_2S_4$ phases produced for the Ba/Fe = 1.100/2.000 starting composition are the same as those for the 1.000/2.000 starting composition, the two isotherms are not entirely equivalent because above the fugacity at which $Ba_{1.100}Fe_2S_4$ is produced, pyrrhotite no longer exists in the products and a barium sulfide phase must appear to balance the excess barium present. X-Ray powder diffraction methods did not reveal which barium sulfide compound was present in the reacted mixtures at this starting composition or at others further away from stoichiometry. However, BaS_3 is likely because it is stable at these temperatures and pressures and is often observed in reacted Ba–Fe–S mixtures, e.g., the reaction mixtures at 650°C.

TABLE III

CONSTANTS FOR THE EQUATION $x = a + b \ln[F(S_2)]$

T (°C)	a	b	
650	0.068(3)	0.0073(8)	
747	0.0904(9)	0.0062(2)	
800	0.081(1)	−0.0119(8)	$f(S_2) \geq 1 \times 10^{-2}$ atm
800	0.131(4)	−0.0010(7)	$f(S_2) \leq 1 \times 10^{-2}$ atm

Note. Standard deviations are in parentheses.

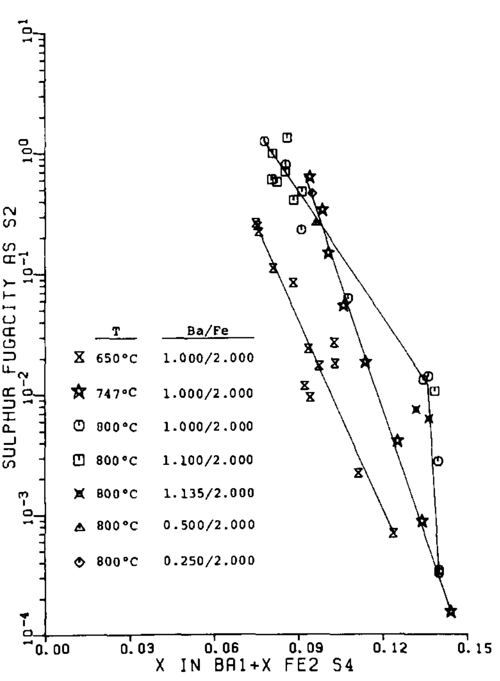

FIG. 4. Lines of best fit for ln $f(S_2)$ vs x for $Ba_{1+x}Fe_2S_4$ at 650, 747, and 800°C.

Discussion

The x vs ln $f(S_2)$ relationship is shown in Fig. 4 for those regions on the $Ba_{1+x}Fe_2S_4$ phase diagram where only one value of x is present. The lines of best fit were obtained from a least-squares determination of the a and b parameters in the equation $x = a + b \ln[f(S_2)]$ and they are listed in Table III. These phases lie at low fugacities and are observed in the regions of Figs. 1–3 where single $Ba_{1+x}Fe_2S_4$ phases are in equilibrium with pyrrhotite phases (or BaS_3 at some starting compositions). It is seen that as $f(S_2)$ increases, the barium concentration, or x, decreases at all temperatures. This is in agreement with Grey's statement (*4*) that the addition of increasing amounts of excess sulfur increases the sulfur pressure in the reaction tube and lowers x. Varying the ratio of Ba/Fe in the starting mixture has no effect on the $Ba_{1+x}Fe_2S_4$–$f(S_2)$ relationship, which implies that any excess iron or barium in the reaction mixture does not affect the $Ba_{1+x}Fe_2S_4$ phase present but is converted to pyrrhotite or barium polysulfide. A most interesting feature of this system becomes evident upon comparison of the three isotherms (Fig. 4). The 650 and 747°C isotherms are linear with only slightly different slopes; however, the value of x at a given $f(S_2)$ and 650°C is always less than the value of x at the same fugacity at 747°C. If the 650°C isotherm is extended into the region between 7×10^{-4} and 1×10^{-4} atm $f(S_2)$ a value of x of about 0.14 is reached. At lower fugacities only $BaFe_2S_3$ would be found. The 800°C isotherm displays two linear regions with a change in slope at approximately 1×10^{-2} atm $f(S_2)$. The break in the $\ln f(S_2)$ vs x curve occurs very near the point at which $BaFe_2S_3$ begins to appear on the 800°C phase diagram. It appears that at high fugacities a limiting value of about 0.072 ± 0.002 is reached for x and $x = 0.142 \pm 0.002$ is the maximum value at low $f(S_2)$.

We conclude that at all reaction temperatures $Ba_{1+x}Fe_2S_4$ phases form a line on the Ba–Fe–S phase diagram which spans the composition range of $x = 0.072$ to $x = 0.142$. Thus every possible composition within these limits attains a fully ordered structure. However, the region between $x = 0$ and $x = 0.072$ is not spanned by phases corresponding to $Ba_{1+x}Fe_2S_4$, but by a biphasic region in which $BaFe_2S_4$ coexists with a phase whose x value is approximately 0.072. This coexistence has also been observed by Nakayama *et al.* (*6*). Using high-resolution electron microscopy they found that $Ba_{1.075}Fe_2S_4$ displays an intergrowth of $BaFe_2S_4$ in the $Ba_{1.075}Fe_2S_4$ matrix. The composition range $0.072 \leq x \leq 0.142$ may be considered an infinitely adaptive series since no biphasic regions exist in this span of phases, but the phase $x = 0$ is not part of it.

Hoggins and Steinfink (*3*) had predicted that the end members of the series might have values $x = 0$ and $\frac{1}{3}$, respectively. The upper limit was based on geometric considerations in which Ba^{2+} was placed into the centers of alternating face sharing square antiprisms and tetragonal prisms. It had been pointed out by Grey (*4*) that systematic variations in Ba–Ba and Fe–Fe distances exist as a function of x. Using the published results as well as our own, the functional dependence $d(\text{Ba–Ba}) = 5.292 - 2.914x$ Å can be obtained, predicting 4.32 Å for Ba–Ba at $x = \frac{1}{3}$. This is considerably shorter than the intermetallic contact 4.44 Å. The $x = 0.140$ phase has Ba^{2+}–Ba^{2+} = 4.88 Å, within 10% of the intermetallic contact, and it appears that this is the physical reason for the upper limit on x. The structure for the lower limit, $x = 0$, was predicted on the basis of the tetrahedral FeS_4 chain orientation in the unit cell observed for $Ba_{10}(Fe_2S_4)_9$ (*2*) and $Ba_9(Fe_2S_4)_8$ (*3*). However, the determination of the crystal structure of $BaFe_2S_4$ showed that the chains of FeS_4 tetrahedra are rotated 90° relative to the predicted structure (*11*). There is, thus, a discontinuity in the framework as x approaches zero. In the $x = 0$ phase Ba^{2+} ions are located at the same z levels as the S^{2-} ions and if the orientation of the tetrahedral chains is maintained as in the $x > 0$ phases, Ba–S distances of about 2.5 Å would result. These are too short and the rotation of the chains gives rise to 3.634 and 3.295 Å distances, those normally observed for this bond.

Conclusion

The infinitely adaptive series of compounds with the formula $Ba_{1+x}Fe_2S_4$ spans the compositions $0.072 \leq x \leq 0.142$. The value of x decreases as the sulfur vapor pressure increases at a given temperature. Control of vapor pressure is essential for the preparation of single-phase material. The Ba^{2+}–Ba^{2+} distance varies inversely with x and is within 10% of the metallic contact at $x = 0.140$. Coulomb repulsion limits x at the upper value. As x decreases toward zero the z parameter of Ba^{2+} changes to bring it into coincidence with the S^{2-} level. If the orientation of the tetrahedral chains remains constant, unrealistically short Ba–S distances are encountered. The lower limit, $x = 0.072$, appears to be determined by this effect.

Acknowledgment

The authors gratefully acknowledge the research support of the National Science Foundation under Grants DMR 76-82092 and DMR 80-05140.

References

1. J. S. Anderson, *J. Chem. Soc. Dalton Trans.*, 1107 (1973).
2. I. E. Grey, *Acta Crystallogr. Sect. B* **31**, 45 (1975).
3. J. T. Hoggins and H. Steinfink, *Acta Crystallogr. Sect. B* **33**, 673 (1977).
4. I. E. Grey, *J. Solid State Chem.* **11**, 128 (1974).
5. J. S. Swinnea and H. Steinfink, *J. Chem. Ed.* **57**, 580 (1980).
6. N. Nakayama, K. Kosuge, and S. Kachi, *J. Solid State Chem.* **36**, 9 (1981).
7. K. C. Mills, "Thermodynamic Data for Inorganic Sulphides, Selenides, and Tellurides," Butterworths, London (1974).
8. H. Rau, T. R. Kutty, and J. R. F. Guedes de Carvalho, *J. Chem. Thermodyn.* **5**, 291 (1973).
9. J. M. Smith and H. C. Van Ness, "Introduction to Chemical Engineering Thermodynamics," 3rd ed., McGraw-Hill, St. Louis (1975).
10. H. Rau, *J. Phys. Chem. Solids* **37**, 425 (1976).
11. J. S. Swinnea and H. Steinfink, *J. Solid State Chem.* **32**, 329 (1980).